Title
AKAP2 anchors PKA with aquaporin-0 to support ocular lens transparency.

Journal
EMBO molecular medicine, 4(1)

ISSN
1757-4676

Authors
Gold, Matthew G
Reichow, Steve L
O'Neill, Susan E
et al.

Publication Date
2012

DOI
10.1002/emmm.201100184

Peer reviewed

EMBO Molecular Medicine

AKAP2 anchors PKA with aquaporin-0 to support ocular lens transparency

*Matthew G. Gold[1†], Steve L. Reichow[2,3†], Susan E. O'Neill[2,3], Chad R. Weisbrod[4], Lorene K. Langeberg[1], James E. Bruce[4], Tamir Gonen[2,3**], John D. Scott[1*]*

Keywords: AKAP; AQP0; cataract; lens; PKA

DOI 10.1002/emmm.201100184

Received August 30, 2011
Revised September 29, 2011
Accepted October 10, 2011

→See accompanying article
http://dx.doi.org/10.1002/emmm.201100188

A decline in ocular lens transparency known as cataract afflicts 90% of individuals by the age 70. Chronic deterioration of lens tissue occurs as a pathophysiological consequence of defective water and nutrient circulation through channel and transporter proteins. A key component is the aquaporin-0 (AQP0) water channel whose permeability is tightly regulated in healthy lenses. Using a variety of cellular and biochemical approaches we have discovered that products of the A-kinase anchoring protein 2 gene (AKAP2/AKAP-KL) form a stable complex with AQP0 to sequester protein kinase A (PKA) with the channel. This permits PKA phosphorylation of serine 235 within a calmodulin (CaM)-binding domain of AQP0. The additional negative charge introduced by phosphoserine 235 perturbs electrostatic interactions between AQP0 and CaM to favour water influx through the channel. In isolated mouse lenses, displacement of PKA from the AKAP2–AQP0 channel complex promotes cortical cataracts as characterized by severe opacities and cellular damage. Thus, anchored PKA modulation of AQP0 is a homeostatic mechanism that must be physically intact to preserve lens transparency.

INTRODUCTION

Approximately 20 million people worldwide suffer from severely reduced vision caused by clouding of the ocular lens known as cataract (Brian & Taylor, 2001). Understanding the environmental and genetic risk factors for cataract is therefore a major global health challenge, which is being aided by basic research of lens physiology. The ocular lens is adapted for optimal focusing of light on the retina. It lacks a conventional vascular system, and its mature fibre cells contain no organelles, which enables minimal light scattering. To accommodate this unusual physiology, the lens has developed an internal circulation system based upon an array of membrane channel and transporter proteins (Mathias et al, 2007). Foremost amongst these is the water channel aquaporin-0 (AQP0), also known as major intrinsic polypeptide (MIP), which constitutes more than 60% of the total membrane protein content of fibre cells (Bloemendal et al, 1972). Consistent with its critical role in the lens, mutation or malfunction of AQP0 causes a loss of lens transparency known as cataract (Berry et al, 2000; Francis et al, 2000; Gu et al, 2007).

Aquaporins form channels for water permeation across biological membranes by virtue of 6-transmembrane helices that assemble a hydrophilic water-conducting pore (Gonen & Walz, 2006). AQP0 serves as a prototype to understand how water channels are regulated at the molecular level (Gonen & Walz, 2006). Three mechanisms reduce AQP0 water permeability. Water channels close when AQP0 tetramers from opposing cells adhere to one another to form adhesive junctions (Gonen et al, 2004). Upon elevation of pH, the de-protonation of His40 and His66 at either end of the pore reduces water flow (Gonen et al, 2004; Nemeth-Cahalan et al, 2004). Binding of

(1) Department of Pharmacology, Howard Hughes Medical Institute, University of Washington School of Medicine, Seattle, WA, USA
(2) Department of Biochemistry, Howard Hughes Medical Institute, University of Washington School of Medicine, Seattle, WA, USA
(3) Current address: Janelia Farm Research Campus, Howard Hughes Medical Institute, Ashburn, VA, USA
(4) Department of Genome Sciences, University of Washington School of Medicine, Seattle, WA, USA
***Corresponding author:** Tel: +1 206 616 3340; Fax: +1 206 616 3386; E-mail: scottjdw@u.washington.edu
****Corresponding author:** Tel: +1 571 209 4238; Fax: +1 571 291 6449; E-mail: gonent@janelia.hhmi.org

†These authors contributed equally to this work.

Ca^{2+}/CaM to a C-terminal cytoplasmic region between residues 225 and 263 of AQP0 decreases water permeability (Varadaraj et al, 2005). Conversely, phosphorylation of AQP0 (Ball et al, 2004) within this regulatory region opens the water pore (Reichow & Gonen, 2008; Rose et al, 2008). However, the intracellular signals and effector molecules that sustain this channel activation event are unknown.

We noted that the residues surrounding Ser235 conform to the protein kinase A (PKA) recognition motif (Zetterqvist & Ragnarsson, 1982). PKA is often sequestered with its substrates by A-kinase anchoring proteins (AKAPs; Coghlan et al, 1995; Scott & Pawson, 2009). Every AKAP contains an amphipathic helix that mediates anchoring of the PKA holoenzyme through interaction with the dimerization and docking (D/D) domain of PKA type II regulatory (RII) subunits (Gold et al, 2006; Kinderman et al, 2006). We reasoned that such an anchoring protein might be a component of the AQP0 complex, so in this study we have explored the role of PKA and AKAPs in regulating AQP0. Biochemical and immunohistochemical experiments show that A-kinase anchoring protein 2 (AKAP2) interacts directly with the C-terminal domain of AQP0 on membranes of outer cortical lens fibre cells. AKAP2 thus anchors PKA in proximity to AQP0, enabling phosphorylation of the water channel at Ser235. The importance of AKAP2 and PKA to AQP0 regulation is underlined by the development of cortical lens cataracts upon incubation of lenses with a cell-permeable peptide that prevents AKAP-mediated PKA anchoring.

RESULTS

AKAP2 is the principal A-kinase anchoring protein in the lens

To identify potential AKAPs in the mammalian lens, sheep lens homogenates were probed with ^{32}P-radiolabelled RII subunits of PKA. Multiple bands ranging in size between 100 and 150 kD were detected using the 'RII overlay' assay (Carr et al, 1992; Fig 1A). Complementary studies used immobilized GST-RII as an affinity ligand to capture lens AKAPs (Fig 1B, lane 2). RII-binding proteins migrating between 100 and 150 kD on SDS–polyacrylamide gel electrophoresis (SDS–PAGE) gels were excised, digested with trypsin and subjected to sequence analysis by mass spectrometry (MS). Peptides corresponding to 22% coverage of AKAP2 (Fig 1C) were assigned on the basis of sequence identity to the bovine ortholog (the sheep proteome is not currently annotated).

Several splice variants are encoded by the AKAP2 gene (Dong et al, 1998). These include a fusion of the membrane associated protein paralemmin-2 and AKAP-KL (Hu et al, 2001). Most, if not all, of these isoforms are enriched in lens extracts as assessed by immunoblot (IB) using antibodies against a common epitope (residues 760–810; Fig 1C and D). Kinase anchoring was demonstrated by the detection of immune complexes formed between AKAP2 and the regulatory (RII) and catalytic (C) subunits of PKA that were absent in IgG controls (Fig 1E, lanes 2 and 3). Also, PKI-sensitive kinase activity towards the Kemptide peptide substrate was enriched 3.6-fold ($n = 3$; $p < 0.001$) following immunoprecipitation with AKAP2 antibody when compared to control IgG (Fig 1F). Taken together, the results in Fig 1 imply that AKAP2 isoforms are the principal AKAPs in the sheep lens.

AKAP2 anchors PKA at cell membranes in the lens outer cortex

The architecture of the mammalian lens is illustrated in Fig 2A. AQP0 is concentrated on the membranes of tightly packed hexagonal fibre cells, where it sustains fluid microcirculation in the absence of a conventional vascular system (Mathias et al, 2007). Immunoblotting of sheep lens fractions demonstrated that AKAP2 is present in the lens cortex (Fig 2B, top panel, lane 3) but is not detected in the lens core (Fig 2B, top panel; lane 2). In contrast, AQP0 is detected in both core and cortical fractions (Fig 2B, bottom panel; lanes 2 and 3). Subcellular fractionation revealed that AKAP2 and AQP0 partition with cortical membranes (Fig 2B, lane 4). However, addition of 1 M NaCl released AKAP2 into the supernatant fraction (Fig 2C, top panel, lane 4), implying that AKAP2 is peripherally attached to cortical membranes via ionic interactions, whereas, AQP0 is an integral membrane protein. Analysis by RII overlay gave consistent results (Fig S1 of Supporting Information).

Immunohistochemical analyses of fixed mouse lenses extend these findings. In axial sections, AKAP2 is detected in the epithelium and outer cortical fibre cells (Fig 2D and F). Its signal is strongest at sites proximal to the equator, as delineated by an inwardly migrating band of nuclei (Fig 2E and F). Equatorial lens sections imaged at higher magnification (40×) reveal that AKAP2 predominates at the plasma membrane in the outer cortex (Fig 2G and J), as indicated by a striated pattern that overlaps with the membrane marker wheat germ agglutinin (WGA; Fig 2H and J). Furthermore, the AKAP2 signal diminishes ~100 μm from the lens surface at the transition zone between the cortex and the core, as demarked by the bow region where lens fibre differentiation begins (Fig 2G and I). At 100× magnification of lens equatorial sections a punctate staining pattern for AKAP2 is discernible (Fig 2K and M) that overlaps with fibre cell membranes (Fig 2L and M). Related studies show that the RII and C subunits of PKA are also present at the same location (Fig S2 of Supporting Information).

AKAP2 binds directly to the C-terminal tail of AQP0

AKAPs often sequester their anchored enzymes with preferred substrates (Smith et al, 2010). Accordingly, AQP0 was enriched in anti-AKAP2 immune complexes (Fig 3A bottom panel, lane 3). Immunofluorescence staining demonstrated a co-distribution of both proteins at the membranes of outer cortical lens fibre cells (Fig 3B–D and Fig S3 of Supporting Information). To identify amino acid determinants that participate in this protein–protein interaction, a series of immobilized AQP0 peptides (20-mers in 2 amino acid increments) that encompass the cytoplasmic tail of the channel were incubated with purified recombinant AKAP2 (Fig 3E and F). Equivalent amounts of each immobilized peptide were confirmed by detection with

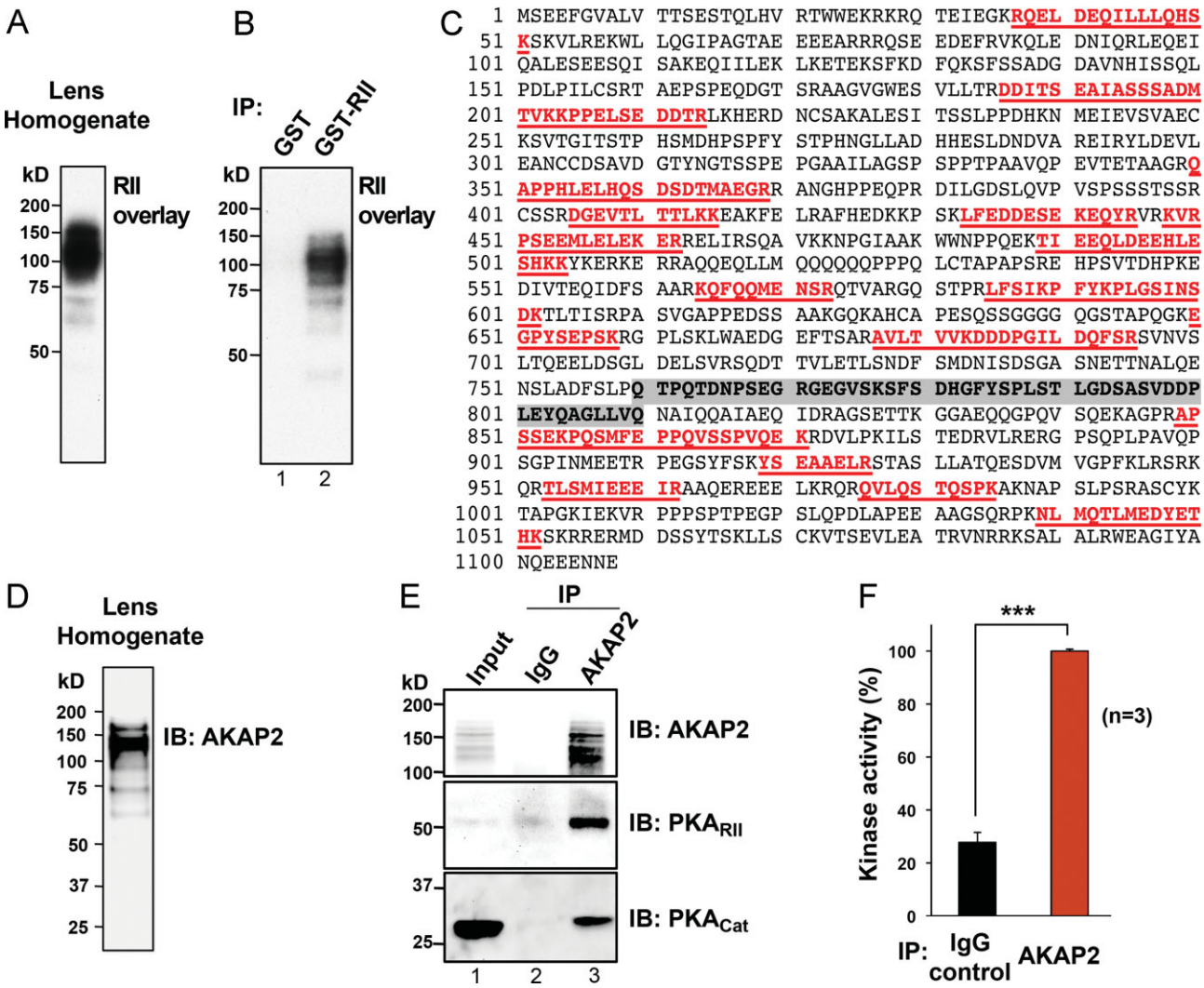

Figure 1. AKAP2 is the predominant lens AKAP.

A. Autoradiograph following ^{32}P-RII overlay of sheep lens homogenate.

B. ^{32}P-RII overlay of lens proteins eluted following addition of PreScission protease to GST (lane 1) and GST-D/D (lane 2) lens immunoprecipitates.

C. Annotated bovine AKAP2 primary sequence. Sheep sequences identified by MS that are identical to the bovine ortholog are underlined in red. The epitope recognized by the anti-AKAP2 antibody is depicted (bold text) in the shaded area.

D. Anti-AKAP2 IB of sheep lens homogenate.

E. Proteins were immunoprecipitated from sheep lens homogenate (input, lane 1) with either rabbit IgG (lane 2) or anti-AKAP2 antibody (lane 3). Co-IP of PKA RII (middle panel) and C (lower panel) subunits is shown by immunoblotting.

F. PKI-sensitive PKA activity in sheep lens homogenate immunoprecipitated with either control rabbit IgG or anti-AKAP2 antibody. Amalgamated data from three experiments are presented.

ultraviolet light (Fig 3F). AKAP2 bound to peptides 3–8 as determined by immunoblotting (Fig 3F). In separate studies, peptide 7, which corresponds to residues 237–256 of AQP0, was used to release native AKAP2 from association with the water channel in solubilized lens homogenates (Fig 3G, lower panel, lane 3), suggesting that a core sequence within this segment of the AQP0 regulatory domain is both necessary and sufficient for AKAP2 binding. A control peptide of identical amino acid composition but scrambled sequence did not prevent co-purification of the AKAP2–AQP0 complex (Fig 3G, lower panel, lane 4). Systematic alanine scanning of the AQP0 237–256 sequence (LKGTRPSESNGQPEVTGEPV) revealed that replacement of Arg241 with alanine eliminated AKAP2 binding, and substitution of the surrounding residues Lys238, Thr240, Glu244 or Asn246 reduced AKAP2 association with the immobilized peptide (Fig 3H). Collectively these biochemical and SPOT array experiments indicate that AKAP2 binds directly to the C-terminus of AQP0, in a manner that involves binding determinants between residues 238 and 246 of the channel.

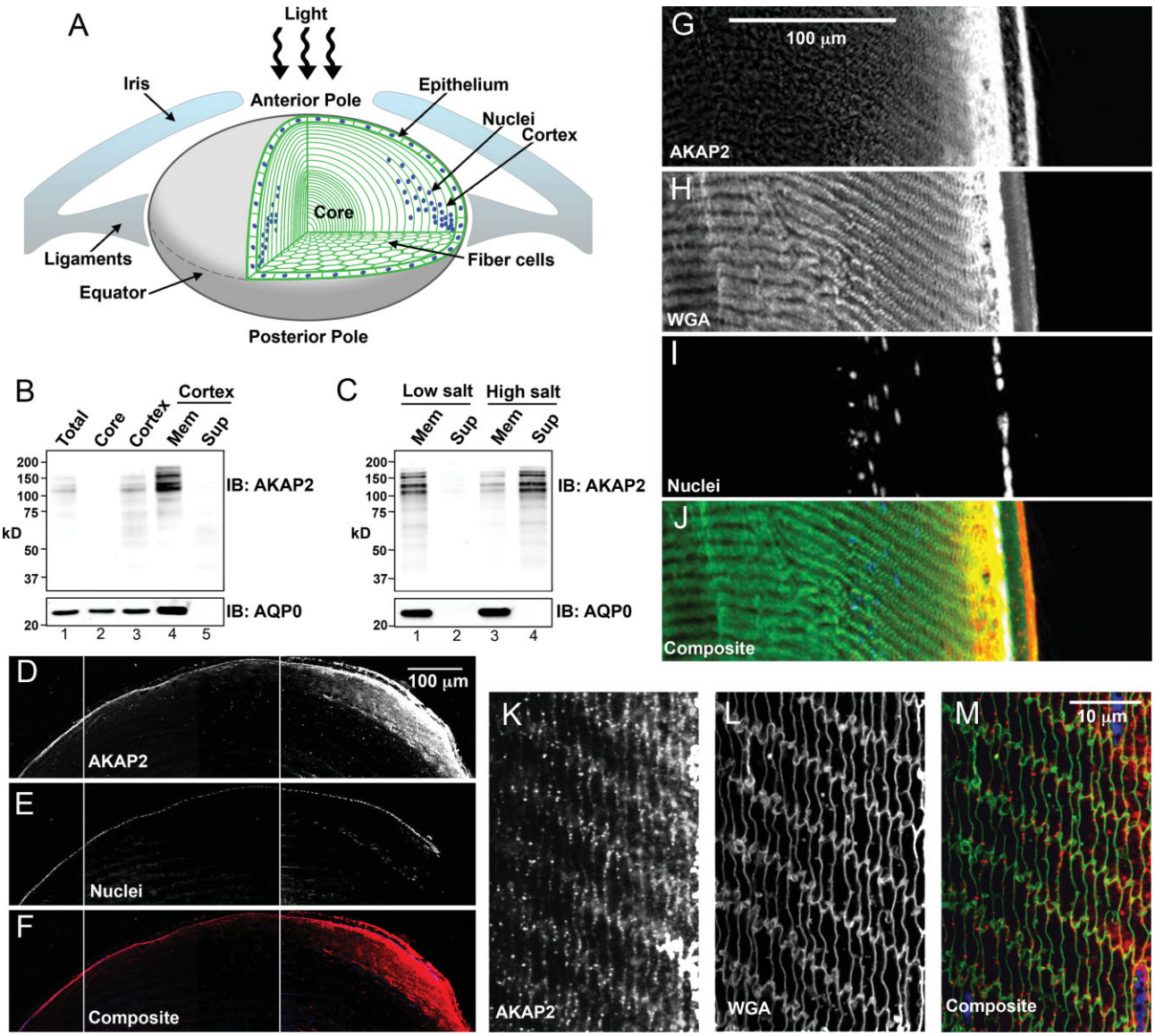

Figure 2. Lens distribution of AKAP2.

A. Schematic of lens cellular architecture. Hexagonal fibre cells are visible in equatorial sections; migrating nuclei at the equator are depicted in axial sections. Epithelial cells are continually generated at the anterior surface and migrate into the outer cortex of the lens at the equator, where they differentiate to fibre cells. Fibre cells develop an elongated hexagonal shape that facilitates packing of neighbouring cells into a lattice. As new fibre cells are added to the cortex, older fibre cells become buried into the core of the lens, where they are terminally differentiated—losing their nuclei and other organelles.

B. Sheep lens homogenate (lane 1) was separated into core (lane 2) and cortex (lane 3). The cortex was subfractionated into membrane (lane 4) and supernatant (lane 5).

C. Cortical membranes were incubated with LLB containing either 0 M NaCl (lanes 1 and 2) or 1 M NaCl (lanes 3 and 4) before subfractionation into membrane (lanes 1 and 3) and supernatant (lanes 2 and 4) fractions. (**B** and **C**) Immunoblotting against AKAP2 (upper panel) and AQP0 (lower panel) is shown for each fraction.

D–F. 10× magnification imaging of axial sections of mouse lens stained with anti-AKAP2 antibody (**D**, red in **F**) and the nuclear marker DRAQ5 (**E**, blue in **F**). Three separate images were aligned to cover the lens from the anterior pole to the equator.

G–J. Immunofluorescence (40×) images of equatorial lens sections are shown following staining with anti-AKAP2 antibody (**G**, red in **J**), membrane marker WGA (**H**, green in **J**) and DRAQ5 (**I**, blue in **J**).

K–M. High-magnification images of equatorial sections of outer lens cortex are shown following staining with anti-AKAP2 antibody (**K**, red in **M**), WGA (**L**, green in **M**) and DRAQ5 (blue in **L**).

PKA prevents AQP0–CaM association through Ser235 phosphorylation

Our mapping studies suggest that AKAP2 could position PKA in a way that favours phosphorylation of AQP0. In keeping with this postulate, the C-subunit of PKA efficiently phosphorylated purified AQP0 in a PKI-sensitive manner (Fig 4A top panel, lanes 2 and 3). MS/MS sequencing of Lys-C-digested AQP0 identified a conserved PKA phosphorylation site at Ser235 in a peptide

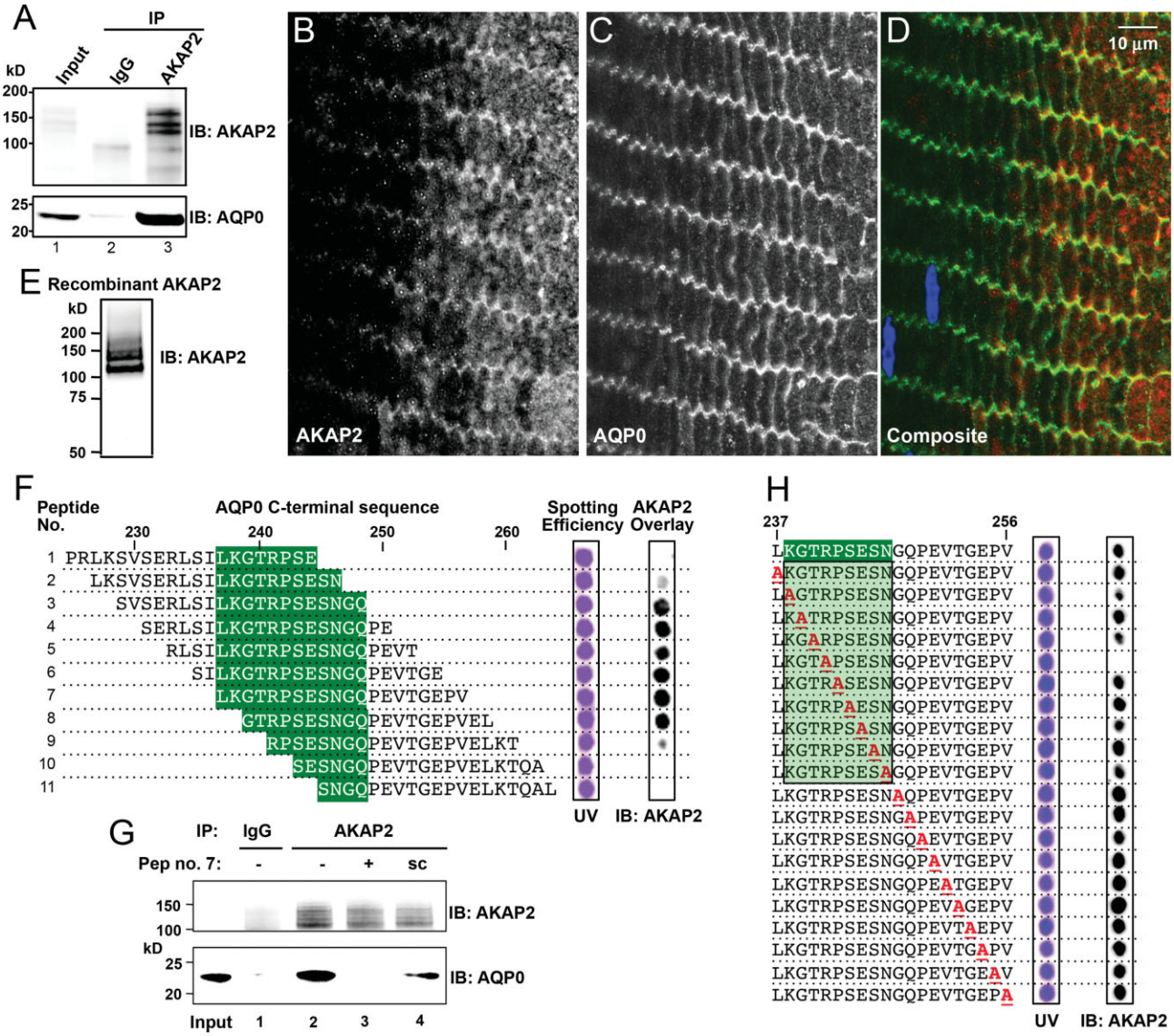

Figure 3. Mapping of AKAP2 binding to AQP0.

A. Proteins from sheep lens homogenate (lane 1) were immunoprecipitated with rabbit IgG (lane 2) or anti-AKAP2 antibody (lane 3). Co-immunoprecipitation of AQP0 was detected by anti-AQP0 IB (lower panel).

B–D. Immunohistochemistry showing co-distribution of AKAP2 (**B**) and AQP0 (**C**) in equatorial lens sections imaged at high magnification. A composite image (**D**) shows AKAP2 (red), AQP0 (green) and DRAQ5 (blue).

E. IB of recombinant AKAP2 produced in bacteria.

F. A series of immobilized 20-mer peptides, moving along the AQP0 sequence in increments of two amino acids in an N- to C- direction from residues 225–263 was synthesized by spot array. Each peptide was coupled to a PEG-amino membrane via the C-terminal carboxyl group. Coupling efficiency was assessed by UV illuminescence (left column). Binding of purified AKAP2 is shown by anti-AKAP2 IB (right column). AKAP2 binding determinants are highlighted in green.

G. Proteins were immunoprecipitated from sheep lens homogenate (input) with either rabbit IgG (lane 1) or anti-AKAP2 antibody (lanes 2–4). Co-IPs were coincubated without peptide (lanes 1 and 2), with WT peptide 7 (lane 3) or with scrambled peptide 7 (lane 4). Co-IP of AQP0 is demonstrated by anti-AQP0 IB in the lower panel.

H. Alanine scanning of a peptide (peptide 7) that spans the AKAP2 binding site. Peptide derivatives were overlaid with purified AKAP2. AKAP2 was detected by IB.

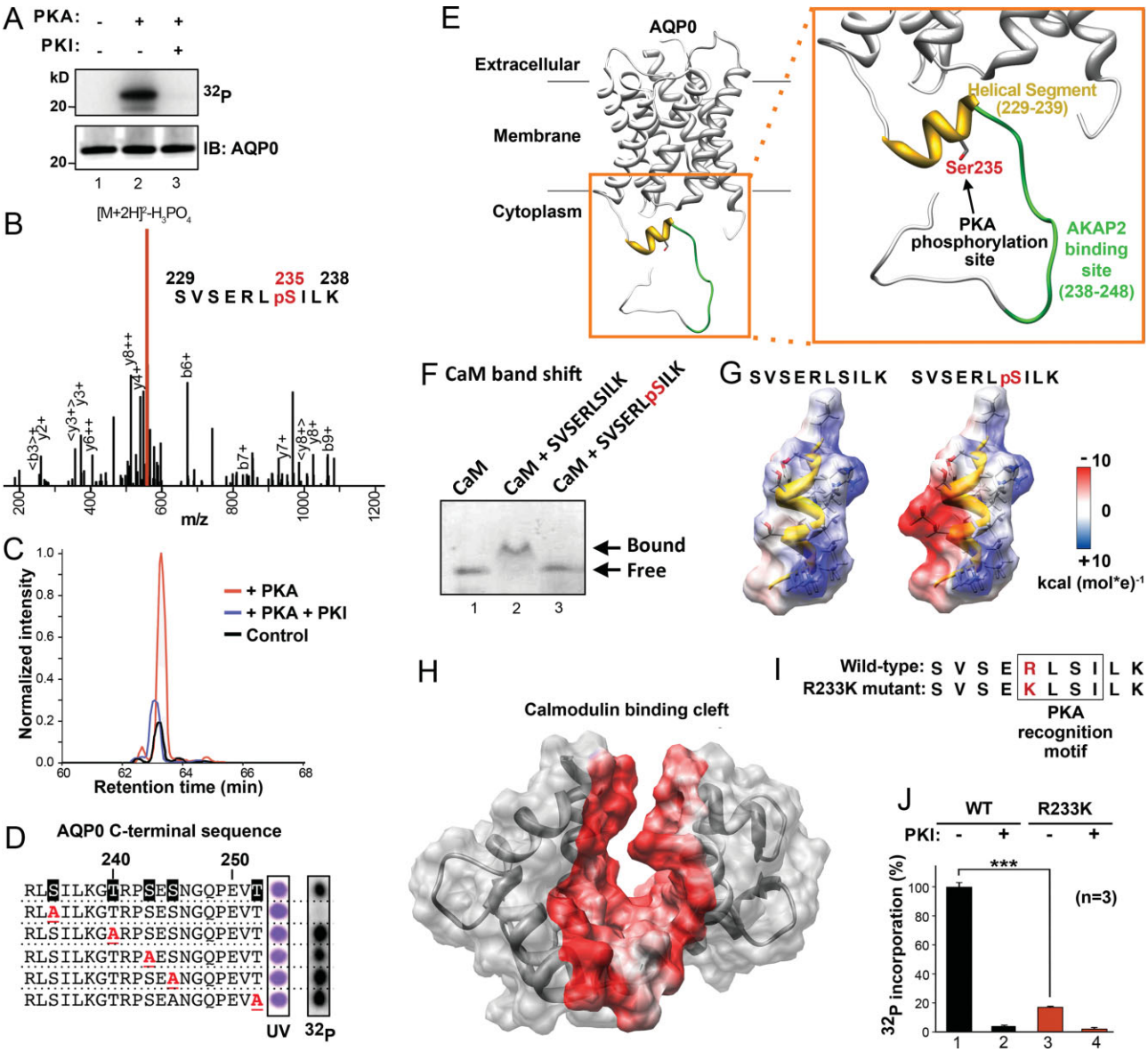

Figure 4. Structural consequence of PKA phosphorylation in AQP0.

A. Autoradiograph (top panel) showing ^{32}P incorporation into purified AQP0 (anti-AQP0 IB, lower panel) following incubation with ^{32}P-γATP +/− PKA C subunit and +/− PKI.

B. Product ion scan of SVSERLpSILK peptide. Neutral loss of H_3PO_4 is strong. A series of γ-H_3PO_4 and β-H_3PO_4 ions were observed enabling determination of the phosphorylation site location at Ser235.

C. Normalized intensity of SVSERLpSILK peptide with retention time during LC following incubation of AQP0 with PKA (red), without PKA (black) and with both PKA + PKI (blue).

D. Autoradiograph (right column) following PKA phosphorylation of arrayed AQP0 233–252 peptides with ^{32}P-γATP. Equal spotting efficiency is demonstrated by UV illuminescence. Each serine and threonine residue was mutated to alanine as indicated.

E. Structural representation using the coordinates of AQP0 (Gonen et al, 2004). Inset: location of the PKA phosphorylation site, AKAP2 binding domain (green) and helical segment (yellow) in the C-terminal domain of AQP0 (PDB ID 2B6P; Gonen et al, 2004).

F. Native gel electrophoresis of CaM alone (lane 1) or in the presence of unphosphorylated (lane 2) or Ser235-phosphorylated (lane 3) AQP0 223–242 peptide.

G. Electrostatic surface representation of the AQP0 C-terminal helix situated between residues 227 and 239 in its unphosphorylated (left) and Ser235-phosphorylated (right) states.

H. Electrostatic surface of the CaM binding cleft.

I. Location of the PKA recognition motif for Ser235 in WT and R233K mutant (Gu et al, 2007) AQP0.

J. Phosphorylation of WT (lanes 1 and 2) and R233K mutant (lanes 3 and 4) AQP0 (223–242) peptides with ^{32}P-ATP was attempted in solution with PKA in the presence (lanes 2 and 4) and absence (lanes 1 and 3) of PKI.

corresponding to residues 229–238 of the channel (Fig 4B and Fig S4 of Supporting Information). Quantitative analysis of the SVSERLpSILK phosphopeptide revealed that Ser235 phosphorylation was increased fivefold in the presence of PKA over untreated AQP0 (Fig 4C). Incubation with PKI diminished this enhancement threefold (Fig 4C). MS detected no other phosphorylation sites in the SVSERLSILK peptide, and follow-up peptide array experiments confirmed that substitution of Ser235 with alanine prevented PKA phosphorylation of AQP0 233–252 peptide (Fig 4D). Furthermore, sequential elimination of other serine or threonine residues within this region had no qualitative effect on phosphate incorporation (Fig 4D).

Inspection of the AQP0 crystal structure (Gonen et al, 2005) reveals that Ser235 is located at the centre of the CaM binding site on AQP0, in a helical segment within ~20 Å of AKAP2 binding determinants (Fig 4E). Band-shift assays using native gel electrophoresis indicate that CaM is capable of binding to AQP0 223–242 (Fig 4F, lane 2), but that Ser235 phosphorylation prevents this interaction (Fig 4F, lane 3). Surface charge analysis reveals complementarities between the charges presented by the AQP0 peptide (Fig 4G) and the reciprocal binding cleft of CaM (Fig 4H). Phosphorylation at Ser235 introduces negative charge at the centre of the AQP0 CaM-binding interface (Fig 4G). Therefore, it is likely that repulsion between like negative electrostatic charges is the basis of decreased CaM binding following PKA phosphorylation at AQP0 residue Ser235. This provides a mechanistic explanation as to why phosphorylation of this region favours the displacement of CaM from AQP0 to open the water pore (Kalman et al, 2008; Reichow & Gonen, 2008; Rose et al, 2008). Independent experiments showed that PKA efficiently phosphorylated an AQP0 peptide bearing Ser235 peptide in solution (Fig 4I and J). Basophilic protein kinases such as PKA recognize arginine or lysine side chains at the *P*-2 position of a substrate recognition sequence (Zetterqvist & Ragnarsson, 1982). Arginine is conserved across species at this position (Arg233; Fig S4 of Supporting Information) in wild-type (WT) AQP0 although a naturally occurring mutation (Gu et al, 2007) introduces a lysine at this position in the channel. Surprisingly, this conservative substitution at position 233 reduced phosphorylation by PKA 5.8-fold ($p < 0.001$; $n = 3$; Fig 4J).

Disruption of A-Kinase anchoring generates outer cortical cataract

Lens transparency is preserved by the constant flow of water carrying with it ions, second messengers and metabolites (Mathias et al, 2007). It has been proposed that circular diffusion patterns are driven by an ionic current that is directed inward at the poles and outward at the equator of the lens and supported by water influx through AQP0 (Donaldson et al, 2010). An alternate model is that water passage through AQP0 gap junctions is sufficient to provide the necessary microcirculation in the lens (Beebe & Truscott, 2010). Irrespective of which fluid circulation model prevails, the phosphorylation of this channel is vital for regulating the rate of water influx. To assess the physiological importance of AKAP–PKA anchoring and AQP0 phosphorylation in maintaining lens transparency, we utilized a cell-permeable disruptor peptide of PKA anchoring (Ht31; Vijayaraghavan et al, 1997), to release the kinase from association with AQP0 *in vivo*. Mouse lenses were incubated in artificial aqueous humour (AAH) in the presence or absence of 10 μM Ht31 (Fig 5A and B). Following 72 h incubation in AAH alone, lens transparency was maintained throughout the lens (Fig 5A). Addition of Ht31 over the same time period led to cataract development in the lens cortex but not the lens core (Fig 5B). Changes in lens opacity were quantified by densitometry (Fig 5C) confirming that displacement of PKA increased development of cortical lens cataracts ($p < 0.001$, $n = 8$). The development of cortical cataracts following disruption of PKA–AKAP interactions is consistent with the cumulative data presented in Figs 1–4.

Immunofluorescence staining of lens sections revealed that the tight hexagonal packing of fibre cells was preserved in control lenses, as shown by membrane staining at low (Fig 5D) and high magnification (Fig 5E and G). RII remained associated with the cell membrane (Fig 5F and G), suggesting that AKAP2-mediated PKA anchoring was preserved under control conditions. In contrast, fibre cell packing in the outer cortex appeared disordered following incubation with Ht31 for 72 h as detected by WGA staining of membranes (Fig 5H). At higher magnification, the catastrophic effects of displacing PKA were more apparent (Fig 5I–K). Many fibre cells are enlarged in a manner that is consistent with intracellular swelling. Moreover, extracellular gaps developed that are indicative of extracellular swelling and tissue architecture breakdown. Additionally, membrane aggregates are present from ruptured cells. Importantly, RII was no longer concentrated at the periphery of fibre cells close to membranes upon treatment with Ht31 (Fig 5I and K). Collectively, the data in Fig 5 argue that the pathological effects on fibre cell swelling and cataract formation may be a consequence of PKA holoenzyme release from AKAP2 in the equatorial cortex of the lens. Accordingly, fluid microcirculation would be seriously interrupted with deleterious effects on lens morphology.

DISCUSSION

We show that AKAP2 is a water-channel-associated anchoring protein that restricts PKA within the immediate vicinity of AQP0 in the equatorial lens cortex. This could likely direct phosphorylation within a regulatory region of AQP0 to modulate water permeability. These findings ascribe the first directly demonstrated function for AKAP2 anchoring proteins. However, a broader implication is that we may have uncovered an unanticipated mechanism for anchored PKA. Our model proposes that anchored PKA may participate in the phosphorylation dependent activation of AQP0 to preserve fluid circulation within the lens. This postulate is substantiated by evidence presented in Fig 5 showing that perturbation of PKA anchoring evokes a pathophysiological state that accentuates the development of cortical cataracts. The involvement of this kinase can now be inferred from pathological mutations in the AQP0 gene (Francis et al, 2000; Gu et al, 2007; Lin et al, 2007). Of

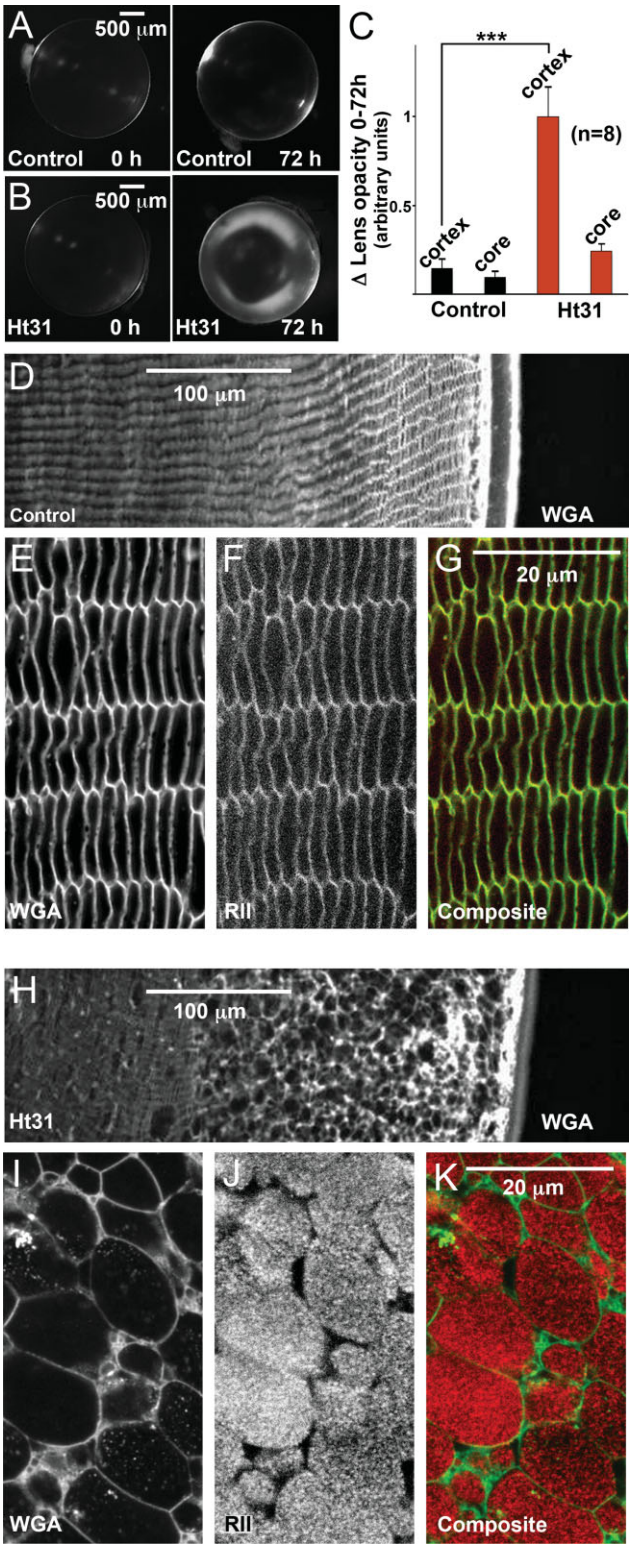

Figure 5. Mislocalization of PKA adversely affects lens transparency.

A–B. Mouse lenses were imaged by dark-field light microscopy before and after 72 h incubation in control conditions (**A**), and in the presence of 10 μM Ht31 (**B**).

C. Quantification of regional changes in lens opacity following 72 h incubations ($n = 8$).

D–G. Images of equatorial sections of lens cortex were collected following 72 h incubation in control conditions. A low-magnification image is shown following staining with WGA (**D**). High magnification images are shown following staining with WGA (**E**, green in **G**) and anti-RII antibody (**F**, red in **G**).

H–K. Equivalent sections are shown following treatment in the presence of 10 μM Ht31. A low magnification image is shown following WGA staining (**H**). High magnification images are shown following staining with WGA (**I**, green in **K**) and anti-RII antibody (**J**, red in **K**).

particular interest is an autosomal dominant cataractogenic mutation that encodes an arginine to lysine substitution at position 233 of AQP0. This corresponds to the *P*-2 position of a PKA phosphorylation site at Ser235 (Zetterqvist & Ragnarsson, 1982). Individuals carrying this mutation exhibit fibre cell swelling, severe light scattering and the early onset of cataracts (Lin et al, 2007). At first glance it may seem surprising that a conservative arginine to lysine mutation reduces phosphorylation of Ser235 to this extent. However, PKA phosphorylation of an AQP0 peptide (residues 223–242) harbouring this R233K mutation was reduced by 5.8-fold ($n = 3$, $p < 0.001$) when compared to the WT sequence (Fig 4H and I). On the basis of these observations we can postulate that mutations that prevent the phosphorylation of Ser 235 favour CaM binding to sustain the closed conformation of the water channel. Hence, we propose that the phosphorylation state of Ser235 has profound effects on AQP0 water permeability.

Two CaM molecules bind per AQP0 tetramer in a cooperative and calcium dependent manner to reduce water conductance (Reichow & Gonen, 2008). Calmodulin (CaM) binds a helical segment located between residues 223 and 242 of each AQP0 protomer. On the basis of our biochemical and cellular data we propose that PKA phosphorylation of Ser235 compromises the electrostatic AQP0–CaM interface to favour the active open state of the water pore. Presumably, the added charge and bulk of a phosphate group at position 235 as depicted in Fig 4G perturbs CaM binding to the regulatory domain of the channel. This allows us to put forward an intriguing new mechanism, whereby, cAMP/PKA phosphorylation must override inhibitory Ca^{2+}/CaM action to permit water conductance through AQP0. One implication of this concept is that bidirectional control of Ser235 phosphorylation would require that the AQP0–AKAP2–PKA complex both has access to cAMP (Alvarez et al, 2003; Goldberg et al, 2004), which can diffuse through gap junctions (Alvarez et al, 2003; Goldberg et al, 2004), and is targeted in proximity to phosphatases. By analogy to other AKAP signalling complexes (Dodge et al, 2001; Dodge-Kafka et al, 2005; Klauck et al, 1996; Tasken et al, 2001), signal termination enzymes for second messenger action may also be binding partners for AKAP2. Although we have not yet investigated the components, complexity or the entire spectrum of AKAP2 binding partners in the lens, it seems reasonable that phosphodiesterases or phosphatases could be recruited to the AKAP2–AQP0 network. In sum, our study charts how a single anchored PKA phosphorylation event that subtly changes the conformation of a key lens membrane protein can be magnified leading to

major pathological effects at the cellular and tissue levels. Interestingly, the water channel AQP0 is only one of several lens proteins that may come under the control of anchored PKA. For example, gap junctions are likewise vital for the circulation system and they are also phosphorylated (Mathias et al, 2010). Conversely, contributing factors to cataract formation in other regions of the lens may include uncontrolled association of crystallins and the formation of high-molecular weight aggregates at the membrane (Mathias et al, 2007). Thus, defects in the PKA–AKAP2–AQP0 axis reported in this article may only represent one of several pathophysiological mechanisms that augment cataract formation.

MATERIALS AND METHODS

Lens fractionation

Lenses were dissected from sheep eyes obtained from the Wolverine Packers slaughterhouse (Detroit, MI). Lenses were decapsulated and fibre cells were homogenized in lens lysis buffer (LLB; 20 mM Tris pH 7.5, 150 mM NaCl, 5 mM EDTA, 5 mM EGTA, 1 mM DTT, 1 mM AEBSF and 1 μM Pepstatin A). The soft cortical tissue was separated from the dense core tissue using a surgical blade. Fibre cell membranes were fractionated from the soluble lysate by ultra-centrifugation at 50,000 g for 30 min. Protein concentrations of lens extracts were determined by BCA (Pierce).

AKAP identification

RII overlay was performed as described previously (Carr et al, 1992). The D/D domain of PKA RIIα (residues 1–45) was cloned into pGEX6P1 enabling expression of GST-D/D with a PreScission protease cleavage site between GST and D/D. Both GST and GST-D/D were expressed in *Escherichia coli* (*E. coli*) BL21 cells and lysed in 25 mM Tris pH 7.5, 500 mM NaCl, 2 mM DTT, 0.5 mM EDTA and 0.1 μg/ml lysozyme prior to purification by affinity to glutathione sepharose (GE Healthcare). Lens lysates were prepared for D/D pulldown experiments by homogenizing sheep lenses in LLB. Lens homogenates were solubilized by supplementing LLB with 1% Triton X-100, followed by sonication for 5 s and centrifugation at 14,000 × *g* for 30 min. Ten millilitres of the resulting supernatant containing 50 mg/ml protein was incubated for 2 h with 200 μl glutathione sepharose beads loaded with 300 μg of either GST or GST-D/D. After 5 × 1 ml washes with LLB with 1% Triton X-100, the beads were incubated overnight with 2 μg PreScission protease (GE Healthcare) in 100 μl LLB with 1% Triton X-100. Eluted proteins were separated by SDS–PAGE, Coomassie-stained and the region of the gel containing proteins of apparent molecular weight between 100 and 130 kD were excised. Proteins were in-gel digested with trypsin, and the resulting peptides were sequenced by Linear Trap Quadrupole Fourier Transform MS. Automated protein identification was performed using the Computational Proteomics Analysis System (Rauch et al, 2006).

Immunoprecipitation

Lens membranes and associated proteins were pelleted from 100 mg homogenized cortical sheep lens by 10 min centrifugation at 14,000 × *g*. Membranes were resuspended in LLB supplemented with 1% Triton X-100, sonicated for 5 s and centrifuged at 14,000 × *g* for 30 min. The supernatant was incubated overnight with 4 μg of either anti-AKAP2 antibody (Novus #61604) or control rabbit IgG. Immune complexes were immunoprecpitated by 1 h incubation with 30 μl Protein A agarose (Promega). IP was also performed in the presence of 5 μg of peptides corresponding to residues 237–256 of sheep AQP0 (w/t: LKGTRPSESNGQPEVTGEPV, scrambled: REVPGKTLSPGGTVPSENEQ). Peptides were synthesized at >95% purity by Biomatik.

PKA activity assay

To quantify PKA activity, immune complexes associated with 30 μl Protein A agarose (as above) were incubated for 1 h with 10 μM cAMP. The resulting elution was split into two, and one half was supplemented with the PKA inhibitor PKI (10 μM). After 10 min, kinase activity +/− PKI was assayed in (50 mM Tris–HCl pH 7.5, 5 mM $MgCl_2$) with 10 μCi/μM (^{32}P-γ) ATP and 1 mM Kemptide (LRRASLG) as substrate. Following 2 h incubation at 30°C, the reactions were spotted onto P81 phosphocellulose paper, which was washed extensively in phosphoric acid and ethanol before scintillation counting. PKI-sensitive activity was calculated in triplicate for both anti-AKAP2 and control rabbit IgG immunoprecipitates.

Lens sectioning and immunohistochemistry

WT 6–8-week-old C57BL/6 mice were euthanized under an atmosphere of CO_2, lenses were dissected and subsequently fixed by overnight incubation with phosphate-buffered saline (PBS) containing 0.75% paraformaldehyde. Fixed lenses were cryoprotected by serial incubations in PBS with 10% (1 h), 20% (1 h) and 30% (overnight) sucrose. Cryoprotected lenses were mounted in Tissue-Tek OCT compound (Sakura Finetek) and 25 μm equatorial sections were taken using a cryostat. Blocking and all antibody incubations were performed in PBS supplemented with 3% w/v BSA and 3% v/v foetal calf serum. The following primary antibodies were used at 2 μg/ml: mouse antibodies to PKA RIIα, RIIβ and C subunits (BD Transduction Laboratories), chicken Anti-AQP0 (Alpha Diagnostic). Anti-AKAP2 antibody was used at 5 μg/ml for immunohistochemistry. The following fluorescent conjugate secondary antibodies (Invitrogen) were used at a dilution of 1–500: Alexa Fluor 488 goat anti-mouse and goat anti-chicken, Alexa Fluor 568 goat anti-rabbit. WGA-FITC conjugate (Sigma–Aldrich) was included simultaneously with secondary antibodies (1:500 v/v). Sections were washed again and mounted on glass slides using ProLong antifade media (Invitrogen). Nuclei were stained by 10 min incubation with a 1:1000 dilution of DRAQ5 (Biostatus) in the final step before mounting. Sections were imaged with a Zeiss LSM 510 META.

Peptide array synthesis and overlays

Peptide arrays were synthesized on PEG-amino membrane using a Multipep (Intavis AG) following the SPOT array procedure. Human AKAP2 (accession BC140818) was purchased from Origene and cloned into the pET15b vector. 6xHis-AKAP2 was purified by affinity to nickel sepharose (Qiagen). For far-Western blots, membranes were blocked in TBS-T supplemented with 5% w/v milk and 1% w/v fatty acid-free BSA.

Assays of AQP0 phosphorylation

To detect PKA phosphorylation of SPOT arrayed AQP0 peptides, membranes were wetted with ethanol and placed in membrane

The paper explained

PROBLEM:

Cataract, or clouding of the ocular lens, is the leading cause of blindness worldwide. Deterioration of lens tissue can occur as a consequence of defective water and nutrient circulation through channel and transporter proteins. A key element of the lens circulatory system is the aquaporin-0 (AQP0) water channel. AQP0 permeability is upregulated by phosphorylation at Ser235 but the intracellular signals and effector molecules that sustain this channel activation event had not previously been identified.

RESULTS:

Protein products of the A-kinase anchoring protein 2 gene (AKAP2/AKAP-KL) bind directly to AQP0 to bring protein kinase A (PKA) into proximity with the water channel. This enables PKA phosphorylation of Ser235 within a calmodulin (CaM)-binding domain of AQP0. The additional negative charge introduced by phosphoserine 235 disrupts electrostatic interactions between AQP0 and CaM thus favouring water influx through the channel. In cultured intact lenses isolated from mice, displacement of PKA from the AKAP2–AQP0 channel complex with a peptide disruptor promotes cortical cataracts as characterized by severe opacities and cellular damage.

IMPACT:

The major implication of this study is that we have uncovered an unanticipated mechanism for anchored PKA in the preservation of fluid circulation within the lens. This notion is consistent with a previously identified cataractogenic mutation in AQP0 that alters the PKA recognition motif for Ser235 phosphorylation. Thus, anchored PKA modulation of water channels in the lens may be an important homeostatic mechanism that maintains lens transparency.

phosphorylation (MP) buffer (20 mM HEPES pH 7.4, 100 mM NaCl, 5 mM $MgCl_2$, 1 mM DTT and 0.2 mg/ml BSA) for 1 h at 20°C. Membranes were blocked overnight in MP supplemented with 1 mg/ml BSA and 100 μM ATP. Phosphorylation was performed in MP containing 10 μCi/μM ^{32}P-γATP and 250 U PKA C subunit (New England Biolabs)/ml for 2 h at 30°C with rocking. Membranes were sequentially washed with 1 M NaCl, 5% phosphoric acid, ethanol, water, before drying and exposure for autoradiography. To obtain purified AQP0, fibre cell membranes were solubilized with 1% decylmaltopyranoside (DM; Anatrace) and purified by both anion exchange using a MonoQ (GE Healthcare) column and subsequently Superdex 200 (GE Healthcare) size exclusion chromatography. Purified AQP0 was concentrated to 0.5 mg/ml in 10 mM HEPES pH 7.0, 50 mM NaCl, 0.3% DM. To test PKA phosphorylation of purified AQP0, 2.5 μg AQP0 was incubated for 1 h in 50 μl MP buffer containing 10 μCi/μM ^{32}P-γATP and supplemented with 250 U PKA C subunit, and 0.1 μg PKI as appropriate. Phosphorylation of AQP0 223–242 (WT and R233K) peptides was performed in the same manner as for PKA phosphorylation of kemptide peptide, but instead using 300 μM AQP0 peptides as substrate.

Phosphoproteomics

Sheep lens membranes were treated for 1 h at 37°C with 200 U calf intestinal phosphatase (New England Biolabs) per 4 mg lens protein prior to purification of AQP0 as described above. Fourteen micrograms of purified AQP0 was incubated overnight at 4°C in 30 μl buffer containing 10 mM HEPES pH 7.0, 50 mM NaCl, 0.3% DM, 10 mM ATP and 10 mM $MgCl_2$. Reactions were supplemented with 0.5 μg PKA C subunit (New England Biolabs) and 1 μg PKI as appropriate. The samples were digested using Lys-C (Sigma–Aldrich) at a 1:50 (w/w) ratio. Lys-C reactions were allowed to proceed for 24 h at 37°C. To remove unwanted buffers and detergent, hydrophobic interaction liquid chromatography (HILIC) was performed using maxi HILIC/SCX spin columns (Nest Group, Southborough, MA), according to the manufacturer's guidelines. No direct phospho-enrichment was performed. The samples were lyophilized and reconstituted in 99.9% water, 0.1% formic acid for liquid chromatography-MS (LC-MS) analysis.

LC was performed using a Waters Nano Acquity UPLC (Waters). Pulled tip columns were constructed in-house using a laser-pulling device (Sutter). A column of 30 cm in length was constructed with 75 μm ID × 360 μm OD fused silica capillary. The packing material used for peptide separation was 100 Å C18 magic beads (Microm Bioresources). A fused silica trap column was constructed from 100 μm ID × 360 μm OD fused silica capillary. The frit was made on one end of the trap with Kasil (PQ) to contain C18 packing material. The packing material used in the trap was 200 Å C18 magic beads (Microm Bioresources). A binary solvent gradient was used for peptide separation. Mobile phase A consisted of 99.9% water with 0.1% formic acid. Mobile phase B consisted of 95% acetonitrile with 0.1% formic acid. The gradient was setup as follows: 1–35% B in 60 min; washing with 80% B for 20 min; and re-equilibration for 20 min using 5% B. MS experiments were conducted on a 7 Tesla dual cell linear ion trap Fourier transform mass spectrometer. The MS method comprised high-resolution precursor Fourier transform ion cyclotron resonance data acquisition (50,000 RP at 400 *m/z*), followed by 20 low-resolution ion trap data acquisitions.

Raw data was converted to mzXML format using ReAdW 4.2.1 (Institute for Systems Biology, Seattle). Initial sequence identification and phopsho-site assignment was performed by Sequest (University of Washington). A precursor tolerance of 25 ppm and a MS/MS ion tolerance of 0.3 Da was applied. Manual analysis of MS/MS patterns were performed to validate phosphorylation site assignment. Peak areas and extracted ion chromatograms were generated using XCalibur 2.0 software (Thermo-Fisher Scientific). Ser235 phosphorylation was compared in the three different conditions

by normalizing the intensity of the SVSERLpSILK phosphopeptide to that of the total ion chromatogram. Extracted ion chromatograms for this phosphopeptide showed excellent agreement and reproducibility in observed retention times, with peaks from all three runs appearing within 30 s (<1% retention time shift) of one another.

Native gel electrophoresis

6His-CaM was purified by affinity to Ni-NTA resin (Qiagen) and Superdex-75 (GE Healthcare) size exclusion chromatography following pET vector-based expression in *E. coli*. Native gel electrophoresis was performed with 5 mg/ml CaM in 50 mM Tris pH 8.0, 5 mM $CaCl_2$ supplemented for 30 min with 1 mg/ml AQP0 223–242 peptides (Anaspec), as appropriate. Protein mobility was imaged by silver stain.

Structural analysis

The coordinates of full-length AQP0 (PDB ID 2B6P; Gonen et al, 2005) and CaM (PDB ID 1CDM; Meador et al, 1993) were analysed. AQP0 residue Ser235 was modelled as phosphoserine to investigate the effect of PKA phosphorylation on the electrostatic surface. Electrostatic surface potentials were calculated and presented using Chimera (Pettersen et al, 2004).

Cataract formation assays

Lenses were dissected from 8- to 10-week-old WT C57BL/6 mice and incubated at 37°C in AAH (125 mM NaCl, 4.5 mM KCl, 10 mM $NaHCO_3$, 2 mM $CaCl_2$, 0.5 mM $MgCl_2$, 5 mM glucose, 20 mM sucrose and 1% penicillin/streptomycin). Lenses that developed cataracts after 6 h in AAH were discarded (~30%). Remaining lenses were incubated with either AAH or AAH supplemented with 10 μM stearated Ht31 (Promega). Lens transparency following 72 h incubations was assessed by dark-field light microscopy. Changes in lens opacity were quantified using ImageJ software (NIH). For cortical opacity, white level intensities (range 1–255) were recorded in 54-pixel boxes evenly spaced around the circumference of each lens at a depth of 100 μm from the surface. The six intensities were averaged and a background intensity, taken from outside of the lens, was subtracted. For core opacity a single measurement was taken at the centre of each lens from which the background intensity was subtracted.

Statistical analysis

All data are presented as the mean ± standard error. Statistical analysis was determined using the unpaired Student *t*-test. A *p*-value of less than 0.05 was considered statistically significant. $^{*}p < 0.05$; $^{**}p < 0.01$; $^{***}p < 0.001$.

Author contributions

MG performed experiments, provided funding, analysed data and wrote the manuscript; SR performed experiments, analysed data and wrote the manuscript; SO performed experiments; CW performed experiments and analysed data; LL analysed data and wrote the manuscript; JB provided funding and analysed the data; TG provided funding, analysed the data and wrote the manuscript; JS provided funding, analysed data and wrote the manuscript.

Acknowledgements

MGG is a Sir Henry Wellcome Postdoctoral Research Fellow. SLR is a Ruth L. Kirchstein National Research Service Award Fellow. The research was funded through NIH grant GM048231 to JDS, and by NIH grants 7S10RR025107, 5R01GM086688 and 5R01RR023334 to JEB. Research in the Gonen laboratory was supported by the American Diabetes Association Career Development award 1-09-CD-05, NIH grants R01GM079233 and U54GM094598 and the Howard Hughes Medical Institute.

Supporting information is available at EMBO Molecular Medicine online.

The authors declare that they have no conflict of interest.

References

Alvarez LJ, Candia OA, Polikoff LA (2003) Beta-adrenergic stimulation of Na(+)-K(+)-2Cl(−) cotransport activity in the rabbit lens. Exp Eye Res 76: 61-70

Ball LE, Garland DL, Crouch RK, Schey KL (2004) Post-translational modifications of aquaporin 0 (AQP0) in the normal human lens: spatial and temporal occurrence. Biochemistry 43: 9856-9865

Beebe DC, Truscott RJ (2010) Counterpoint: the lens fluid circulation model—a critical appraisal. Invest Ophthalmol Vis Sci 51: 2306-2310; discussion 2310–2302

Berry V, Francis P, Kaushal S, Moore A, Bhattacharya S (2000) Missense mutations in MIP underlie autosomal dominant 'polymorphic' and lamellar cataracts linked to 12q. Nat Genet 25: 15-1517

Bloemendal H, Zweers A, Vermorken F, Dunia I, Benedetti EL (1972) The plasma membranes of eye lens fibres. Biochemical and structural characterization. Cell Differ 1: 91-106

Brian G, Taylor H (2001) Cataract blindness—challenges for the 21st century. Bull World Health Org 79: 249-256

Carr DW, Stofko-Hahn RE, Fraser ID, Cone RD, Scott JD (1992) Localization of the cAMP-dependent protein kinase to the postsynaptic densities by A-kinase anchoring proteins. Characterization of AKAP 79. J Biol Chem 267: 16816-16823

Coghlan VM, Perrino BA, Howard M, Langeberg LK, Hicks JB, Gallatin WM, Scott JD (1995) Association of protein kinase A and protein phosphatase 2B with a common anchoring protein. Science 267: 108-111

Dodge KL, Khouangsathiene S, Kapiloff MS, Mouton R, Hill EV, Houslay MD, Langeberg LK, Scott JD (2001) mAKAP assembles a protein kinase A/PDE4 phosphodiesterase cAMP signaling module. EMBO J 20: 1921-1930

Dodge-Kafka KL, Soughayer J, Pare GC, Carlisle Michel JJ, Langeberg LK, Kapiloff MS, Scott JD (2005) The protein kinase A anchoring protein mAKAP coordinates two integrated cAMP effector pathways. Nature 437: 574-578

Donaldson PJ, Musil LS, Mathias RT (2010) Point: a critical appraisal of the lens circulation model—An experimental paradigm for understanding the maintenance of lens transparency? Invest Ophthalmol Vis Sci 51: 2303-2306

Dong F, Feldmesser M, Casadevall A, Rubin CS (1998) Molecular characterization of a cDNA that encodes six isoforms of a novel murine A kinase anchor protein. J Biol Chem 273: 6533-6541

Francis P, Berry V, Bhattacharya S, Moore A (2000) Congenital progressive polymorphic cataract caused by a mutation in the major intrinsic protein of the lens, MIP (AQP0). Br J Ophthalmol 84: 1376-1379

Gold MG, Lygren B, Dokurno P, Hoshi N, McConnachie G, Tasken K, Carlson CR, Scott JD, Barford D (2006) Molecular basis of AKAP specificity for PKA regulatory subunits. Mol Cell 24: 383-395

Goldberg GS, Valiunas V, Brink PR (2004) Selective permeability of gap junction channels. Biochim Biophys Acta 1662: 96-101

Gonen T, Walz T (2006) The structure of aquaporins. Q Rev Biophys 39: 361-396

Gonen T, Sliz P, Kistler J, Cheng Y, Walz T (2004) Aquaporin-0 membrane junctions reveal the structure of a closed water pore. Nature 429: 193-197

Gonen T, Cheng Y, Sliz P, Hiroaki Y, Fujiyoshi Y, Harrison SC, Walz T (2005) Lipid–protein interactions in double-layered two-dimensional AQP0 crystals. Nature 438: 633-638

Gu F, Zhai H, Li D, Zhao L, Li C, Huang S, Ma X (2007) A novel mutation in major intrinsic protein of the lens gene (MIP) underlies autosomal dominant cataract in a Chinese family. Mol Vis 13: 1651-1656

Hu B, Copeland NG, Gilbert DJ, Jenkins NA, Kilimann MW (2001) The paralemmin protein family: identification of paralemmin-2, an isoform differentially spliced to AKAP2/AKAP-KL, and of palmdelphin, a more distant cytosolic relative. Biochem Biophys Res Commun 285: 1369-1376

Kalman K, Nemeth-Cahalan KL, Froger A, Hall JE (2008) Phosphorylation determines the calmodulin-mediated Ca^{2+} response and water permeability of AQP0. J Biol Chem 283: 21278-21283

Kinderman FS, Kim C, von Daake S, Ma Y, Pham BQ, Spraggon G, Xuong NH, Jennings PA, Taylor SS (2006) A dynamic mechanism for AKAP binding to RII isoforms of cAMP-dependent protein kinase. Mol Cell 24: 397-408

Klauck TM, Faux MC, Labudda K, Langeberg LK, Jaken S, Scott JD (1996) Coordination of three signaling enzymes by AKAP79, a mammalian scaffold protein. Science 271: 1589-1592

Lin H, Hejtmancik JF, Qi Y (2007) A substitution of arginine to lysine at the COOH-terminus of MIP caused a different binocular phenotype in a congenital cataract family. Mol Vis 13: 1822-1827

Mathias RT, Kistler J, Donaldson P (2007) The lens circulation. J Membr Biol 216: 1-16

Mathias RT, White TW, Gong X (2010) Lens gap junctions in growth, differentiation, and homeostasis. Physiol Rev 90: 179-206

Meador WE, Means AR, Quiocho FA (1993) Modulation of calmodulin plasticity in molecular recognition on the basis of X-ray structures. Science 262: 1718-1721

Nemeth-Cahalan KL, Kalman K, Hall JE (2004) Molecular basis of pH and Ca^{2+} regulation of aquaporin water permeability. J Gen Physiol 123: 573-580

Pettersen EF, Goddard TD, Huang CC, Couch GS, Greenblatt DM, Meng EC, Ferrin TE (2004) UCSF Chimera—a visualization system for exploratory research and analysis. J Comput Chem 25: 1605-1612

Rauch A, Bellew M, Eng J, Fitzgibbon M, Holzman T, Hussey P, Igra M, Maclean B, Lin CW, Detter A, *et al* (2006) Computational Proteomics Analysis System (CPAS): an extensible, open-source analytic system for evaluating and publishing proteomic data and high throughput biological experiments. J Proteome Res 5: 112-121

Reichow SL, Gonen T (2008) Noncanonical binding of calmodulin to aquaporin-0: implications for channel regulation. Structure 16: 1389-1398

Rose KM, Wang Z, Magrath GN, Hazard ES, Hildebrandt JD, Schey KL (2008) Aquaporin 0-calmodulin interaction and the effect of aquaporin 0 phosphorylation. Biochemistry 47: 339-347

Scott JD, Pawson T (2009) Cell signaling in space and time: where proteins come together and when they're apart. Science 326: 1220-1224

Smith FD, Langeberg LK, Cellurale C, Pawson T, Morrison DK, Davis RJ, Scott JD (2010) AKAP-Lbc enhances cyclic AMP control of the ERK1/2 cascade. Nat Cell Biol 12: 1242-1249

Tasken KA, Collas P, Kemmner WA, Witczak O, Conti M, Tasken K (2001) Phosphodiesterase 4D and protein kinase a type II constitute a signaling unit in the centrosomal area. J Biol Chem 276: 21999-22002

Varadaraj K, Kumari S, Shiels A, Mathias RT (2005) Regulation of aquaporin water permeability in the lens. Invest Ophthalmol Vis Sci 46: 1393-1402

Vijayaraghavan S, Goueli SA, Davey MP, Carr DW (1997) Protein kinase A-anchoring inhibitor peptides arrest mammalian sperm motility. J Biol Chem 272: 4747-4752

Zetterqvist O, Ragnarsson U (1982) The structural requirements of substrates of cyclic AMP-dependent protein kinase. FEBS Lett 139: 287-290

